

# Thermal Energy Storage Using Horizontal Shell-Tube Heat Exchanger: Numerical Investigation on Temperature Variation of HTF

Fajar Anggara\*, Rinasa Agistya Anugrah\*\*‡, Hadi Pranoto\*

\*Department of Mechanical Engineering, Engineering Faculty, Universitas Mercu Buana, Jalan Meruya Selatan No.1, Jakarta Indonesia

\*\*Department of Mechanical Engineering, Faculty of Vocational Program, Universitas Muhammadiyah Yogyakarta, Jalan Brawijaya, Tamantirto, Kasihan, Bantul, Yogyakarta 55183 Indonesia

(fajar.anggara@mercubuana.ac.id, rinasaanugrah@umy.ac.id, hadi.pranoto@mercubuana.ac.id)

‡ Corresponding Author; Fajar Anggara, Jalan Meruya Selatan No.1, Tel: +62215840816,

Fax: +62215840816, fajar.anggara@mercubuana.ac.id

*Received: 03.09.2019 Accepted: 12.11.2019*

**Abstract-** Latent Heat Thermal Energy Storage (LHTES) is a method to store thermal energy in a Phase Change Material (PCM). Due to the higher energy density, the efficiency of the size of the container might happen. However, the thermal energy storing (charging) time on LHTES is considerably inefficient. The increasing velocity of HTF was conducted using a modified fin and encapsulation to improve the charging time. Similarly, with this motivation, numerical analysis with modified density modelling was conducted to investigate the effect of temperature of heat transfer fluid (HTF) on PCM. This investigation was validated with shell-tube geometry experiment. The experiment set-up was divided into two parts where shell part used as circulation of Heat Transfer Fluid (HTF) and tube part containing PCM (RT-52). This simulation carried out using ANSYS FLUENT 17 to observe evolution on radial-axial temperature, melting time, melting contour and natural convection as the effect of HTF temperature variation. The natural convection got higher and induced the circulation in tube as well. Thus, the melting area was much more at the top cylinder. Melting time decreased significantly as the rising of HTF temperature.

**Keywords** Thermal Energy Storage, Phase Change Material, Numerical Analysis, Natural Convection, Temperature Effect.

## 1. Introduction

The tendency of using fossil energy has been suppressed to decrease due to environmental issue and scarcity. In other side the growth of population each year impose high demand energy with annual consumption of oil reached 1.7 tons[1]. By regarding the environmental issue, scarcity of energy source and high demand energy to withstand these issues, the way out is to leverage renewable energy. Many researches have been developed to achieve this goal such as using wave energy[2][3], supplementary energy by using photovoltage (PV)[4], and energy saving and storage [5].

Latent Heat Thermal Energy Storage (LHTES) is vital in saving and supply energy demand, especially in thermal

energy. LHTES becomes very popular on energy storage applications because of high energy density, wide range temperature operation, constant temperature operation and high density[6]. Despite that, the time consumed on charging process is inefficient due to low thermal conductivity.

As a result, many efforts had been conducted to improve melting time, including using finned container [7]–[9], nano particle[10][11], transposable PCM [12] and porous material [13].

Numerical analysis was conducted to observe melting phenomena in various geometry to improve the charging process. In such an effort, simulation has a vital role in overcoming limited time and budget in the experiment[14]

[15]. Some of the numerical analyses had been conducted primarily in the vertical [16], [17] in 2-D, and horizontal orientation 3-D [18].

During searching on the literature on the effect of temperature of HTF on PCM has been conducted using numerical analysis [19][20][21]. According to these previous works gave same result by increasing temperature on HTF would decrease the melting time, and with the assumption PCM properties are constant. In this study, the observation of melting phenomena with HTF variation is conducted, but the density of PCM depends on its phase especially on horizontal orientation and using a shell-tube heat exchanger. 3-D simulation was carried out to see melting phenomena and the temperature evolution in the radial and axial direction. Density modelling could be engaged by using a user-defined function in ANSYS FLUENT 17.

## 2. Material Characteristics

In this simulation, PCM used is paraffin wax RT-52 in which the density depends on its phase. Although the chemical reaction applications in the simulation. PCM selection was crucial, and it had to suit the working range especially in the term of temperature range and chemical reaction between component. The thermal properties of PCM tabulated in Table 1[18].

**Table 1.** PCM properties Paraffin Wax RT-52

Properties	Value
Melting range	49 – 53 °C
Heat Storage Capacity	173 kJ/kg
Density Solid (15°C)	880 kg/m <sup>3</sup>
Density Liquid (80°C)	760 kg/m <sup>3</sup>
Volume expansion	16%
Heat Conductivity	0.2 W/(m°K)
Kinematic viscosity (80°C)	31.28 x 10 <sup>-6</sup> m <sup>2</sup> /s
Specific Capacity	2 kJ/kgK

## 3. Numerical Model and Simulation

Governing equation to simulate melting phenomena is using enthalpy porosity, where enthalpy inserted into mass, energy and momentum equations. In such of that the calculation of the energy, mass and momentum balance between cell using enthalpy form to accommodate phase change in melting and solidification phenomena [22]. The governing equations described as follow [23]:

Mass continuity equation

$$\frac{\partial \rho H}{\partial t} + \nabla \cdot (\rho \vec{V}) = 0 \quad (1)$$

Momentum equation:

$$\frac{\partial \rho v}{\partial t} + \nabla \rho v \vec{V} = -\nabla P + \mu \cdot \nabla^2 v + \rho g - S \quad (2)$$

Denoting  $\rho$  was density,  $\mu$  was dynamic of viscosity, and  $S$  represented source porosity that mimic the melting and solidification phenomena.  $S$  is described in the following equation:

$$S = \frac{(1-f)^2}{f^3 - \epsilon} A_{mush} \vec{V} \quad (3)$$

$A_{mush}$  was the mushy-zone parameter represented the pseudo porosity medium and it was defined as  $10^7$ .  $f$  was indicated as liquid-fraction of PCM and it is related to the porosity. When the cell is fully solidified the porosity becomes zero, and it described as follows:

$$f = \begin{cases} 0 & T < T_{solidus} \\ \frac{T - T_{solidus}}{T_{liquidus} - T_{solidus}} & T_{solidus} \leq T \leq T_{liquidus} \\ 1 & T > T_{liquidus} \end{cases} \quad (4)$$

PCM melted above liquidus temperature or molten when the temperature was between solidus and liquidus. Otherwise, it was solid if the temperature below solidus temperature. Where  $\alpha_l$  and  $\alpha_s$  were the density at the liquid and solid phase, respectively. Corresponding density to the phase as follows:

$$\alpha = f\alpha_l + (1-f)\alpha_s \quad (5)$$

The equation of energy is described as follows:

$$\frac{\partial \rho H}{\partial t} + \nabla \rho H V = \nabla \cdot (k \nabla T) \quad (6)$$

According to [24] pressure velocity coupling scheme, simple and piso has no difference when they are compared to that experiment, but this simulation uses coupled scheme since convergency is faster to achieve. The discretization method for pressure is PRESTO and for the rest using second-order upwind.

### 3.1. Geometry and Mesh Type

The setting of the geometry in this simulation was the same as an experimental set-up. Shell-tube heat exchanger concept used in which two cylinders installed concentrically with different diameters. Figure 3.1. showed the smaller one used as tube and the big one as a shell.

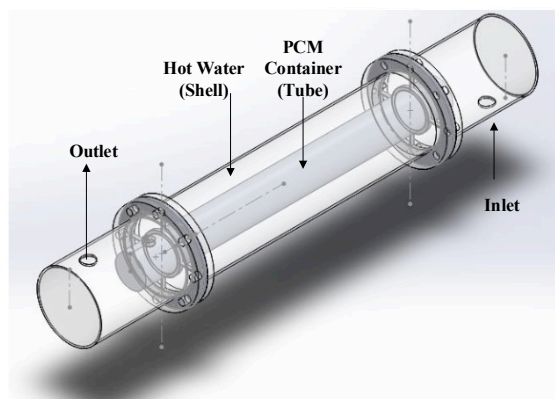


**Fig.3.1.** The geometry of the experiment

In this simulation, the mesh generated in Gambit was hex mesh. The mesh is shown in Fig.3.2.

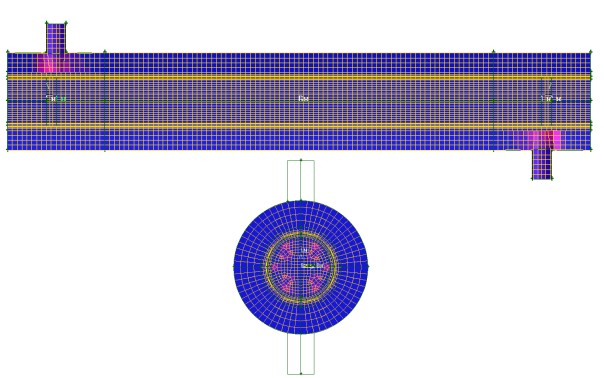


**Fig.3.2.** Meshing

Some of part of the geometry were excluded in the simulation due to mesh quality. However, the result of the simulation was not affected, and it showed a proper validation. The worst skewness and aspect ratio of mesh are 0.587 and 25.38 respectively.

**3.2. Experimental Set-Up**

HTF flowed into the inlet at the bottom and out to outlet at the top of the shell. Due to the limitation of the apparatus of the experiment, HTF temperature could not be higher than 90°C, and it varied at 60°C, 75°C, and 90°C.

Figure.3.3. showed the position of thermocouple where temperature data was obtained. Axial temperature position obtained at T3, T6, T7, T8 while in radial position at T1, T2, T3, T4, T5. HTF flow rate was maintained at 4L/min until PCM melted completely.

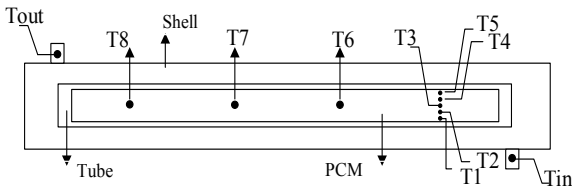


**Fig.3.3.** Position of thermocouple

**4. Result and Discussion**

In this session, the discussion will focus on the result of this work starting with validation of simulation, describing the melting contour, explaining the effect of temperature variation on temperature evolution.

Validation convinces the validity of simulation that is shown on the independency of mesh, then comparing the temperature graph to the experiment in radial and axial direction. The effect of natural convection will be obviously appeared on melting contour and evolution of temperature in radial and axial direction.

**4.1. Validation**

This session of validation started with independency of mesh. Figure.4.1. shows independency of mesh with 144000 has slightly different to 300000 and 500000. In such that, the number of mesh used in this simulation is 144000.

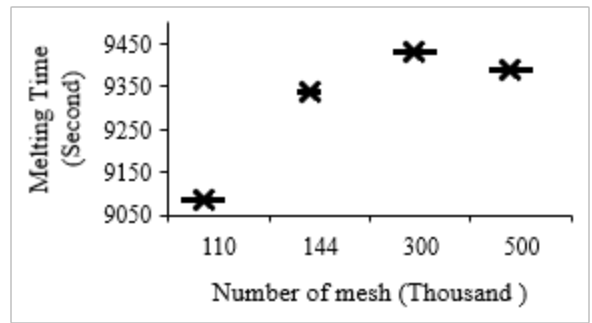


**Fig.4.1.** Independency of mesh

After showing the independency of mesh, the next validation was conducted by comparing temperature evolution on the graphic between simulation and experiment. Figure.4.2 and Figure.4.3. showed the comparison on the graphic at 60°C in a radial and axial direction.

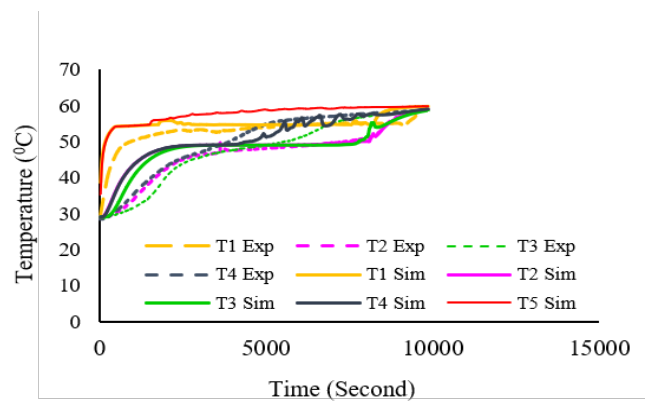


**Fig.4.2.** Comparison of radial temperature

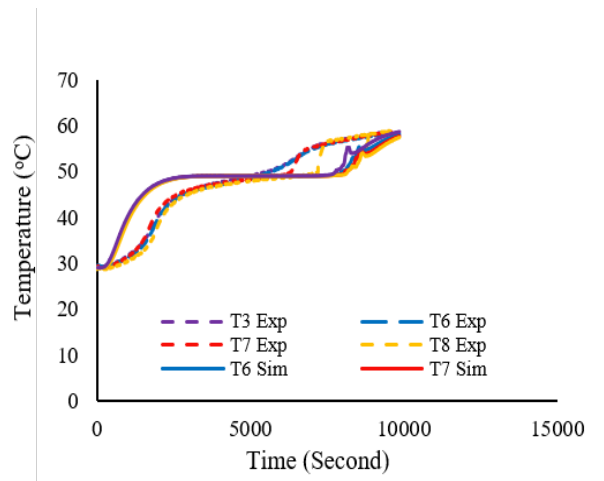


**Fig.4.3.** Comparison of axial temperature

In terms of this validation, it had been investigated in the previous paper. It presented various validations such as melting contour, the average coefficient correlation between graph of temperature simulation and experiment in radial and axial direction is 0.76, the deviation of melting time was less than 5%. The validation showed this simulation had a good agreement. Tweaking parameters such as mushy-zone on the previous paper was used in this simulation.

### 5. The Effect of Temperature Variation

In this session, the impact of temperature variation was presented. As mentioned earlier, the effect of this variation is included on melting contour, melting time and temperature evolution in radial and axial direction.

#### 5.1. Melting Contour

In the Fig.5.1. showed liquid fraction on melting contour in a radial position at 1020 second. At the same time, with the higher HTF temperature, the amount of melting area was much more.

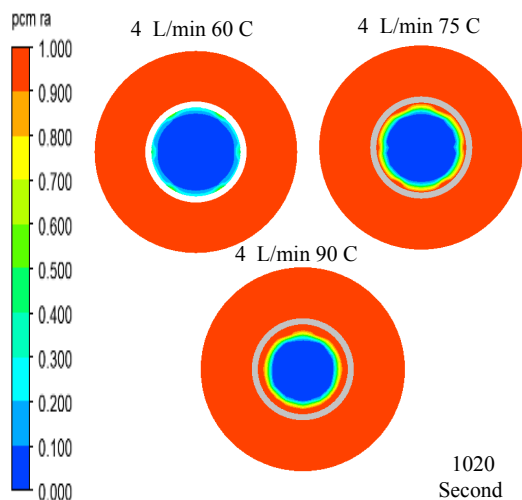


**Fig.5.1.** The melting contour in radial position at 1020 second

Symmetry melting contour occurred in the Fig.5.1. at the temperature of 60°C and 75°C. It indicated the effect of natural convection was not significant. On the other hand, natural convection was taken into account at temperature 90°C as the top of the cylinder had much more melting area than bottom one. This effect gradually increased when the amount of molten layer near the tube wall also increased.

#### 5.2. Melting Time

Investigation of melting time affected the temperature variation described in the Fig.5.2. It showed that heat flux through the wall tube is increased. As a result, the melting time decreased at the higher temperature of HTF.

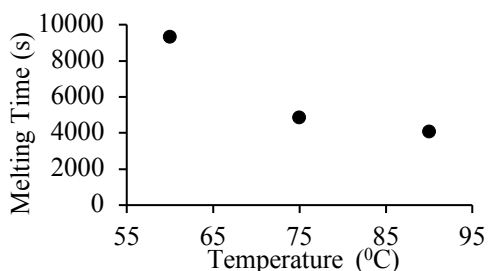


**Fig.5.2.** The effect of temperature variation to melting time

#### 5.3. Temperature Evolution

It has been described that melting time decreased by increasing HTF temperature. It could be shown in the Fig.5.3 that the curve with higher temperature is relatively shorter in the abscissa. However, the distribution of heat in radial and axial direction has not been clearly described. To describe how the temperature distribution in such direction, the temperature evolution has been plotted in Fig. 5.4. and Fig.5.5.

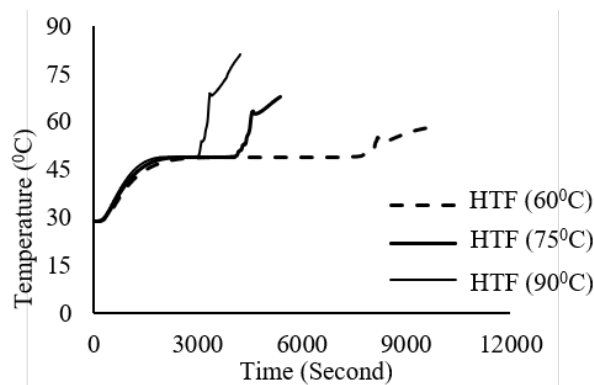


**Fig.5.3.** Comparison of T3

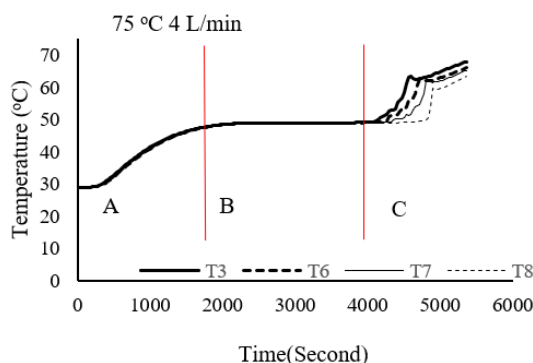


**Fig.5.4.** Temperature evolution in the axial direction

Figure.5.4. showed temperature evolution in axial direction. In Figure.5.4, the temperature evolution was divided into three regions such as A, B, and C where sensible and latent heat take place. In region A, PCM was in solid phase in which the thermal conductivity had a significant impact on temperature distribution. Since PCM was homogenous, the distribution of temperature in radial position was nearly the same.

In region B, the distribution of temperature in radial direction is nearly the same, and it has a constant temperature. In term of a constant temperature, it follows that latent heat attempts to change in PCM phase from solid to liquid.

Another case in region C, the temperature has significant increase near the side of inlet. In such a way of that the accumulation of heat is much more at the near side of inlet. Hence, T3 experiences significant increasing in C region.

The effect of natural convection in tube cylinder could be observed in Fig.5.5. Although T1 and T5 had same position of close to the wall, temperature on T5 was higher than T1 because of the natural convection. Due to natural convection, forcing the heat flow in the tube cylinder tends to reach the top position of the tube. The present of this circulation was due to gradient density where the lower density tends to enter upper area as shown in Fig.5.6.

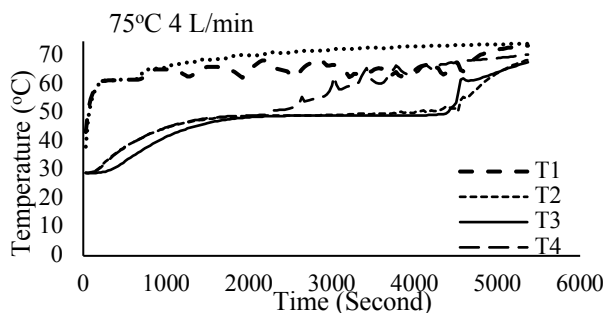


Fig.5.5. Temperature evolution in the axial direction

Thus, there was a circulation flow that inhibited the melting rate at the bottom position. It implied that the temperature near top area was higher than bottom one. Similarly the temperature of T4 was more elevated than T2 and T3.

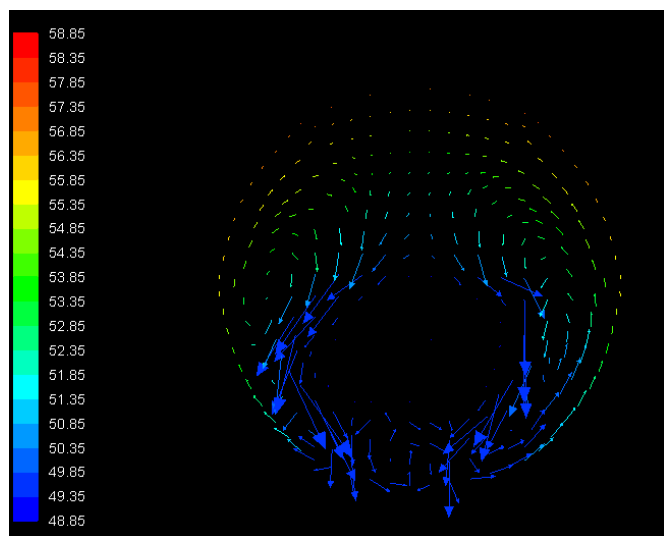


Fig.5.6. Vector of velocity temperature at 60°C

Vector of velocity temperature in Fig.5.6. showed the circulation due to gradient density. The other effect of natural convection is inducing the fluctuation on T1 and T5 in temperature graph and it is shown in the Fig.5.7.

This fluctuation is corresponded to the velocity vector in the Fig.5.6. This velocity tends to get higher as the increasing of HTF temperature inlet.

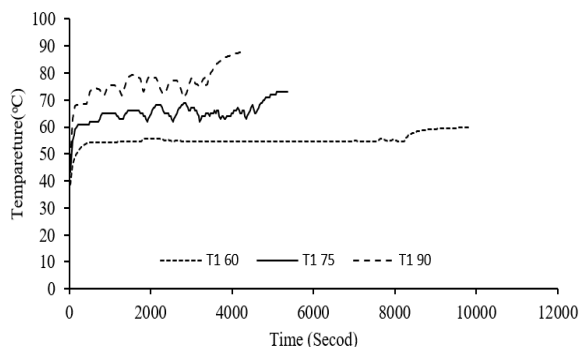


Fig.5.7. Comparison of T1

## 6. Conclusions

3-D shell-tube heat exchanger model was simulated using ANSYS FLUENT 17 with user-defined function to model the behaviour of PCM. The result shows an excellent agreement to the experiment. This numerical analysis has been carried out as didactic method to engage deep understanding of melting phenomena.

The effect of natural convection due to gradient density was more significant when the circulation flow in the tube gradually increased. This circulation was a driven force to engage the melting area at the top cylinder became much more than bottom one. The other effect of natural convection is corresponded to the velocity that caused the fluctuation in temperature graph. Another underlined case was the accumulation of heat flux depending on the driven force that present in tube and how close the container to HTF inlet.

User-defined was a vital role in capturing the behaviour of natural convection in PCM. So, it was wide open to study the modelling of PCM to mimic its response at the experiment.

Especially in this experiment, there were no sinking phenomena of PCM captured in this simulation. This phenomenon was still vague, and it needed more literature whether it happened in the experiment or due to the disturbance.

## References

- [1] H. Abdelkader, A. Meriem, C. Ilhami, and K. Korhan, "Smart grid and renewable energy in Algeria," *2017 6th Int. Conf. Renew. Energy Res. Appl. ICRERA 2017*, vol. 2017-January, pp. 1166–1171, 2017.
- [2] A.S. Deborah, M. Bryan, L. Marcus, G. Rachael, K. Bryant, M. Brooke, M.K. Daniel, "Two-Stage Monte Carlo Simulation to Forecast Levelized Cost of Electricity for Wave Energy," *2017 6th Int. Conf. Renew. Energy Res. Appl. ICRERA 2017*, vol. 2017-January, pp. 5–8, 2017.
- [3] T. Manabu, A. Ashraful, K. Yoichi, Y. Kohei, O. Shinya, N. Shuich, "Performance Analysis of Counter-Rotating Impulse Turbine for Wave Energy

- Conversion,” *Turbomachinery, 2017 6th Int. Conf. Renew. Energy Res. Appl. ICRERA 2017*, vol. 2017-January, pp. 222–228, 2017.
- [4] I. Keskin and G. Soykan, “Reduction of peak power consumption by using photovoltaic panels in Turkey,” *2017 6th Int. Conf. Renew. Energy Res. Appl. ICRERA 2017*, vol. 2017-Janua, pp. 886–890, 2017.
- [5] A. Zurfi, G. Albayati, and J. Zhang, “Economic feasibility of residential behind-the-meter battery energy storage under energy time of-use and demand charge rates,” *2017 6th Int. Conf. Renew. Energy Res. Appl. ICRERA 2017*, vol. 2017-Janua, no. 1, pp. 842–849, 2017.
- [6] M. A. Taher and M. N. Fares, “Experimental investigation of solar energy storage using paraffin wax as thermal mass,” *Int. J. Renew. Energy Res.*, vol. 7, no. 4, pp. 1752–1766, 2017.
- [7] M. Parsazadeh and X. Duan, “Numerical study on the effects of fins and nanoparticles in a shell and tube phase change thermal energy storage unit,” *Appl. Energy*, vol. 216, no. February, pp. 142–156, 2018.
- [8] J. M. Mahdi, S. Lohrasbi, D. D. Ganji, and E. C. Nsofor, “Accelerated melting of PCM in energy storage systems via novel configuration of fins in the triplex-tube heat exchanger,” *Int. J. Heat Mass Transf.*, vol. 124, pp. 663–676, 2018.
- [9] K. A. Aly, A. R. El-Lathy, and M. A. Fouad, “Enhancement of solidification rate of latent heat thermal energy storage using corrugated fins,” *J. Energy Storage*, vol. 24, no. May, p. 100785, 2019.
- [10] S. Ebadi, S. H. Tasnim, A. A. Aliabadi, and S. Mahmud, “Melting of nano-PCM inside a cylindrical thermal energy storage system: Numerical study with experimental verification,” *Energy Convers. Manag.*, vol. 166, no. January, pp. 241–259, 2018.
- [11] R. P. Singh, H. Xu, S. C. Kaushik, D. Rakshit, and A. Romagnoli, “Effective utilization of natural convection via novel fin design & influence of enhanced viscosity due to carbon nano-particles in a solar cooling thermal storage system,” *Sol. Energy*, vol. 183, no. October 2018, pp. 105–119, 2019.
- [12] N. H. S. Tay, M. Liu, M. Belusko, and F. Bruno, “Review on transportable phase change material in thermal energy storage systems,” *Renew. Sustain. Energy Rev.*, vol. 75, no. November 2016, pp. 264–277, 2017.
- [13] X. Yang, S. Feng, Q. Zhang, Y. Chai, L. Jin, and T. J. Lu, “The role of porous metal foam on the unidirectional solidification of saturating fluid for cold storage,” *Appl. Energy*, vol. 194, pp. 508–521, 2016.
- [14] B. Y. Prawira and C. Soekardi, “Analisis Aliran Uap Pada Nozzle Tip Sampling Probe Pltp Menggunakan Computational Fluid Dynamics,” *Sinergi*, vol. 21, no. 3, p. 213, 2017.
- [15] P. David, “Terhadap Fenomena Fluidisasi Dalam Fluidized Bed Dengan Menggunakan Cfd,” *Sinergi*, vol. 20, no. 3, pp. 239–243, 2016.
- [16] M. Longeon, A. Soupart, J. F. Fourmigué, A. Bruch, and P. Marty, “Experimental and numerical study of annular PCM storage in the presence of natural convection,” *Appl. Energy*, vol. 112, pp. 175–184, 2013.
- [17] S. Motahar and R. Khodabandeh, “Experimental study on the melting and solidification of a phase change material enhanced by heat pipe,” *Int. Commun. Heat Mass Transf.*, vol. 73, pp. 1–6, 2016.
- [18] F. Anggara, J. Waluyo, T. A. Rohmat, Fauzun, I. Pranoto, Suhanan, M. Nadjib, P. R. Ansyah, “Simulation and validation of PCM melting in concentric double pipe heat exchanger,” *AIP Conf. Proc.*, vol. 2001, 2018.
- [19] F. Benmoussa, A. Benzaoui, and H. Benmoussa, “Thermal behavior of latent thermal energy storage unit using two phase change materials: Effects of HTF inlet temperature,” *Case Stud. Therm. Eng.*, 2017.
- [20] K. Panchabikesan, M. V. Swami, V. Ramalingam, and F. Haghighat, “Influence of PCM thermal conductivity and HTF velocity during solidification of PCM through the free cooling concept – A parametric study,” *J. Energy Storage*, 2019.
- [21] Z. Li and Z. G. Wu, “Analysis of HTFs, PCMs and fins effects on the thermal performance of shell-tube thermal energy storage units,” *Sol. Energy*, vol. 122, pp. 382–395, 2015.
- [22] A. A. Al-Abidi, S. Bin Mat, K. Sopian, M. Y. Sulaiman, and A. T. Mohammed, “CFD applications for latent heat thermal energy storage: A review,” *Renew. Sustain. Energy Rev.*, vol. 20, pp. 353–363, 2013.
- [23] ANSYS Inc. (US), “Ansys Users’ Guide,” *Aging (Albany. NY)*, vol. 7, no. 11, pp. 956–963, 2015.
- [24] H. Shmueli, G. Ziskind, and R. Letan, “Melting in a vertical cylindrical tube: Numerical investigation and comparison with experiments,” *Int. J. Heat Mass Transf.*, vol. 53, no. 19–20, pp. 4082–4091, 2010.